

# Ferroelectric Behavior of $\text{Pb}(\text{Mg}_{1/3}\text{Nb}_{2/3})\text{O}_3$ (PMN) Obtained by the Sol–Gel Method

Purificación Escribano,<sup>\*,†</sup> Héctor Beltrán,<sup>†</sup> Eloisa Cordoncillo,<sup>†</sup>  
Germà García-Belmonte,<sup>‡</sup> Luisa Ruiz,<sup>§</sup> José M<sup>a</sup> González-Calbet,<sup>§</sup> and  
Anthony R. West<sup>||</sup>

*Departamento de Química Inorgánica y Orgánica and Departamento de Ciencias Experimentales, Universitat Jaume I, 12080 Castellón, Spain, Departamento de Química Inorgánica, Facultad de Químicas, Universidad Complutense, 28040 Madrid, Spain, and Department of Engineering Materials, University of Sheffield, Mappin Street, Sheffield S1 3JD, United Kingdom*

Received June 29, 2000. Revised Manuscript Received October 25, 2000

The ferroelectric behavior of lead magnesium niobate perovskite, obtained by sol–gel methods, has been investigated in three samples with compositions based on  $\text{Pb}(\text{Mg}_{1/3}\text{Nb}_{2/3})\text{O}_3$  (PMN) to which an excess of PbO and MgO has been added. Electron probe microanalysis (EPMA) showed a single phase of stoichiometry  $\text{PbMg}_{0.33}\text{Nb}_{0.68}\text{O}_{3.02}$  in sample 2,  $\text{PbMg}_{0.36}\text{Nb}_{0.69}\text{O}_{3.09}$  in sample 3, and  $\text{PbMg}_{0.32}\text{Nb}_{0.67}\text{O}_3$  together with PbO in sample 4. Permittivity measurements reach values higher than 22 000 for sample 2 and 11 000 for samples 3 and 4. A microstructural characterization of the first two samples, by means of high-resolution electron microscopy, shows the presence of small domains of double periodicity inserted in a matrix with a single cubic perovskite structure. The concentration of double domains is higher in the first sample. The third sample shows a mixture phase due to the presence of PbO. The relationship between microstructure and electrical behavior shows that the permittivity values are related not only to the existence of a single PMN phase but also to Pb:(Mg + Nb) ratios close to 1 and Mg:Nb ratios close to 0.5.

## Introduction

Lead magnesium niobate,  $\text{Pb}(\text{Mg}_{1/3}\text{Nb}_{2/3})\text{O}_3$  (PMN), is an important relaxor ferroelectric material that exhibits a high dielectric constant and a high electrostrictive strain coefficient. X-ray diffraction studies are in agreement with an average cubic  $\text{ABO}_3$  perovskite [space group (S.G.)  $Pm\bar{3}m$ ], at room temperature, which would involve Mg and Nb atoms randomly distributed on the B sites.<sup>1,2</sup> However, selected area electron diffraction (SAED) and high-resolution transmission electron microscopy (HRTEM) studies<sup>3,4</sup> reveal the existence of microdomains, showing a 2-fold perovskite superstructure, inserted in a cubic matrix. Such microdomains could proceed from Mg and Nb ordering, within a rich Nb matrix.

The dielectric properties of complex lead-based perovskite materials, with the general formula  $\text{Pb}(\text{B}'_x\text{B}''_{1-x})\text{O}_3$ , depend on B-sites ordering. If these sites are randomly occupied, a normal ferroelectric behavior,

with sharply defined Curie transition temperatures, is observed. However, a relaxor ferroelectric is obtained if cations are ordered. Dielectric constants unusually high are observed over a wide temperature range for these relaxor materials. The temperature at which the dielectric constant is maximal shifts to higher values and decreases when frequency increases. In relaxor ferroelectrics, structural disorder in B-sites has been proposed to disrupt the translational crystal symmetry, giving an apparent anisotropic component for some measured electrical properties.<sup>5–7</sup>

Several techniques have been used to study the local B-site distortions providing atomic-level explanations for the high dielectric properties of PMN: (a) long-range B-site distortions may occur causing deviations from cubic crystal symmetry at low temperature and (b) short-range B-site changes involving off-center shifts or movement in the B-sites. These structural changes seem to be responsible for local positive and negative charge separation in these materials that creates a bulk spontaneous polarization. In addition, HRTEM,<sup>8</sup> EXAFS,<sup>9</sup> and single-crystal X-ray diffraction<sup>10</sup> studies have shown the presence of domains due to a partially ordered

\* To whom correspondence should be addressed.

<sup>†</sup> Departamento de Química Inorgánica y Orgánica, Universitat Jaume I.

<sup>‡</sup> Departamento de Ciencias Experimentales, Universitat Jaume I.

<sup>§</sup> Universidad Complutense.

<sup>||</sup> University of Sheffield.

(1) Bonneau, P.; Garnier, P.; Husson, E.; Morell, A. *Mater. Res. Bull.* **1989**, *24*, 201.

(2) Smolenskii, G. A.; Siny, I. G.; Pisarev, R. V.; Kuzminov, E. G. *Ferroelectrics* **1976**, *12*, 135.

(3) Husson, E.; Chubb, M.; Morell, A. *Mater. Res. Bull.* **1988**, *23*, 357.

(4) Chen, J.; Chan, H. M.; Harmer, M. H. *J. Am. Ceram. Soc.* **1989**, *72*, 593.

(5) Glazer, A. M.; Mabud, S. A. *Acta Crystallogr.* **1978**, *B34*, 1060.

(6) Gupta, S. M.; Kulkarni, A. R. *Mater. Chem. Phys.* **1994**, *39*, 98.

(7) Zhukov, S. G.; Chernyshev, V. V.; Aslanov, L. A.; Vakhrushev, S. B.; Schenk, H. *J. Appl. Crystallogr.* **1995**, *28*, 385.

(8) Bursill, L. A.; Qian, H.; Peng, J.; Fan, X. *Physica B* **1995**, *216*, 1.

(9) Ye, Z. G. *Ferroelectrics* **1996**, *184*, 193.

(10) Prouzet, E.; Husson, E.; de Mathan, N.; Morell, A. *J. Phys. Condens. Matter* **1993**, *5*, 4889.

distribution of  $\text{Mg}^{2+}$  and  $\text{Nb}^{5+}$  ions that leads to local regions of variable Mg/Nb ratio: (i) negatively charged domains with Mg/Nb mole ratio 1:1 and (ii) positively charged Nb-rich domains.<sup>11</sup>

Previous spectroscopic studies, however, have not provided a complete understanding of the role of the short-range B-site ordering in the overall structure of PMN that can provide an atomic-level explanation for the relaxor ferroelectric behavior. Conclusions about the short-range B-site ordering from these investigations have been controversial. Recent static  $^{93}\text{Nb}$  NMR measurements for single crystals of PMN show both fast- and slow-relaxing components. This behavior has been interpreted as inconsistent with the predicted 1:1 ordered Mg/Nb model for PMN.<sup>12</sup> Although large charge fluctuations have been predicted for the 1:1 model, no evidence has been found by XPS.<sup>13</sup> Such results, however, indicated that the cation ordering in the B-site has a more complex nature and that the Mg and Nb ions are more likely randomly distributed. Depero and Sangaletti<sup>14</sup> also proposed several new structural models for PMN based on computer simulations of detailed X-ray reflection data, suggesting that an average long-range cubic lattice structure for PMN is consistent with X-ray reflection data, with a possible intergrowth of tetragonal and rhombohedral phases. However, such an intergrowth is only consistent with the temperature dependence for the long-range local B-site cation ordering in PMN materials.

Electron paramagnetic resonance (EPR) is an important spectroscopic technique for examining the short-range ordering in PMN powders prepared from different solid-state synthetic methods and for PMN/PbTiO<sub>3</sub> (PT) solid solution materials. Huang et al.<sup>15</sup> have observed that the appearance and intensities of the EPR signals vary with temperature and are also dependent on synthetic route.

In this sense, we have recently synthesized PMN by means of a simple sol-gel method at room temperature.<sup>16</sup> Compositional changes were observed during the process, and finally three samples with slight compositional variations from the ideal stoichiometry ( $\text{Pb}(\text{Mg}_{1/3}\text{Nb}_{2/3})\text{O}_3$ ) were obtained. In this paper, we discuss the electrical behavior of these samples as a function of the microstructural characterization performed by means of SAED and HRTEM.

### Experimental Section

Three samples of compositions: 59% PbO, 24% MgO, 17% Nb<sub>2</sub>O<sub>5</sub>; 56% PbO, 29% MgO, 15% Nb<sub>2</sub>O<sub>5</sub>; and 48% PbO, 40% MgO, 12% Nb<sub>2</sub>O<sub>5</sub> (mol %) named **2**, **3**, and **4**, respectively, have been prepared according to the experimental procedure described in ref 16. X-ray diffraction patterns corresponding to samples **2**, **3**, and **4** could be indexed on the basis of a single cubic PMN phase (space group *Pm3m*). Chemical compositions

obtained by EPMA are very close to that expected for ideal PMN,  $\text{PbMg}_{0.33}\text{Nb}_{0.68}\text{O}_{3.02}$ , and  $\text{PbMg}_{0.36}\text{Nb}_{0.69}\text{O}_{3.09}$  in samples **2** and **3**, respectively. However, PbO was detected in sample **4** in addition to the majority  $\text{PbMg}_{0.32}\text{Nb}_{0.67}\text{O}_3$  phase.

Permittivity measurements, both real  $\epsilon'$  and imaginary  $\epsilon''$  parts, have been performed at several stimulus frequencies, keeping the temperature fixed. This procedure allows the determination of the permittivity spectrum, by means of which a complete dielectric characterization is reached. Samples have been placed in a cryogenic chamber that permits the control of the temperature between 77 and 350 K. The impedance meter (Hewlett-Packard HP4128) programmed in the frequency range from 100 Hz to 1 MHz completes the experimental setup. For these electrical measurements, an organopaste and gold electrodes were applied to the surfaces of the pellets fired at 800 °C.

SAED and HRTEM have been carried out on two electron microscopes: (i) JEOL 2000FX fitted with a double tilting goniometer stage ( $\pm 45^\circ$ ) and (ii) JEOL 4000EX with a double tilting goniometer stage ( $\pm 25^\circ$ ), respectively.

### Results and Discussion

Figure 1 shows the behavior of the permittivity (real and imaginary parts) as a function of temperature for the three PMN samples. In the case of the real part (Figure 1a), permittivity presents, as expected for this type of material, a high degree of frequency dispersion below the maximum temperature ( $T_{\text{max}} \approx 270$  K, depending on the stimulus frequency). Above this temperature, frequency dispersion is clearly reduced and the temperature coefficient of permittivity  $d\epsilon'/dT$  is reached at a very low value. On the other hand, the imaginary part of the permittivity, which accounts for the dielectric losses, also shows a peak around  $T_{\text{max}}$  and decreases at both high and low temperatures (Figure 1b). Both facts indicate the relaxor character of the PMN samples. However, different values of permittivity at low frequencies (100 Hz) measured at  $T_{\text{max}}$  between samples **2**, **3**, and **4**, respectively, can be observed. Whereas permittivity reaches values as high as 22 000 for sample **2**, only values around 11 000 are exhibited for samples **3** and **4**.

To explain the above behavior, permittivity spectra for all samples at  $T = 253$  K were studied (Figure 2).  $\epsilon'$ , as a function of frequency, steeply increases from high to low frequencies in all three samples, as expected in the case of frequency dispersion. In addition,  $\epsilon''$  shows the low-frequency part of a broadened relaxation peak, whose maximum is observed at  $\approx 300$  kHz in sample **2** and should lie outside the measuring frequency range for samples **3** and **4**. As is observed, low-frequency slope  $n$  of  $\epsilon''$  spectra exhibits very low values, a clear indication of the non-Debye feature of the relaxation process. It must be stressed that the analyzed samples present the same pattern of frequency spectrum. In all three cases, only a clearly distinct relaxation process is sufficient for explaining this polarization mechanism. Strictly speaking, Figure 2 shows the low-frequency wing of this process. Other possible electrical contributions such as dc conductivity, grain boundary effects, or different phase responses do not appear in the frequency spectra and therefore should be precluded in a proper explanation. We can conclude that differences in the measured dielectrical behavior among samples must be ascribed to different features of the bulk PMN material.

Current models of the ferroelectric relaxor mechanism are based on the existence of dipolar domains on the

(11) Zhang, Q. M.; You, H.; Mulvihill, M. L.; Jang, S. J. *Solid State Commun.* **1996**, *97*, 693.

(12) Glinchuk, M. D.; Bykov, I. P.; Laguta, V. V. *Ferroelectrics* **1993**, *143*, 39.

(13) Parmigiani, F.; Rollandi, L.; Samoggia, G.; Depero, L. E. *Solid State Commun.* **1996**, *100*, 801.

(14) Depero, L. E.; Sangaletti, L. *Solid State Commun.* **1997**, *102*, 615.

(15) Huang, J.; Chasteen, N. D.; Fitzgerald, J. J. *Chem. Mater.* **1998**, *10*, 3848.

(16) Beltrán, H.; Cordoncillo, E.; Escribano, P.; Carda, J. B.; Coats, A.; West, A. R. *Chem. Mater.* **2000**, *12*, 400.

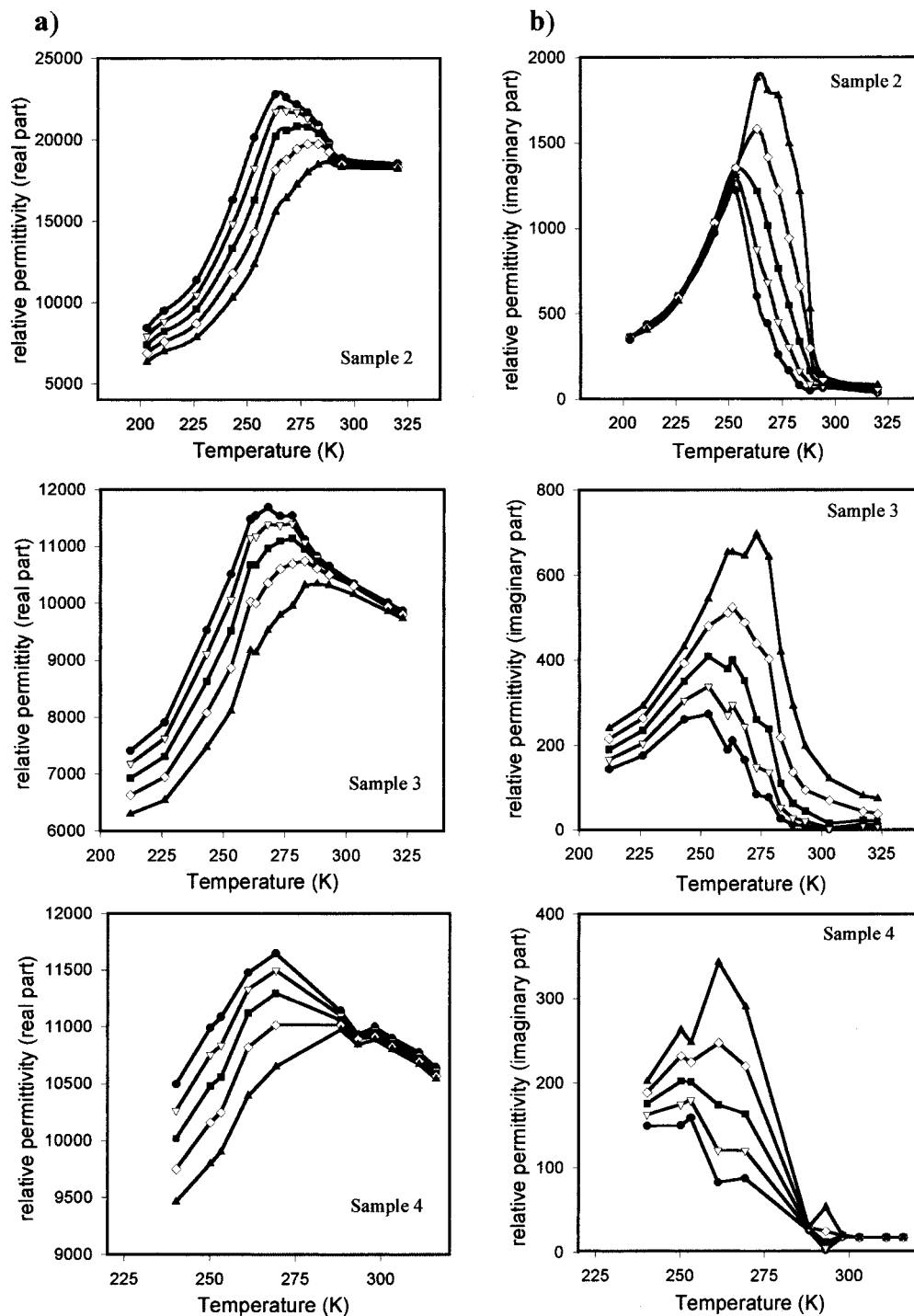


**Figure 1.** Permittivity as a function of temperature: (a) real part and (b) imaginary part. Frequencies: (●) 100 Hz, (▽) 1 kHz, (■) 10 kHz, (◇) 100 kHz, and (▲) 1 MHz.

nanometric scale. Studies by neutron and X-ray diffraction on PMN-based relaxors have revealed rhombohedral distortion in the lattice related to clusters of Mg and Nb cations. These polar clusters, distributed in size, can also vary their size as a function of temperature. Viehland et al.<sup>17</sup> have emphasized the influence of the cluster size on the width of the relaxation characteristic time. They showed that spherical clusters of diameter 45 and 55 Å would have relaxation frequencies of

approximately  $2 \times 10^7$  and  $2 \times 10^3$ , respectively. Taking this idea into account, Lu and Calvarin<sup>18</sup> proposed that an exponential distribution of polar volumes  $V$ , between the critical limit of the crystalline cell  $V_c$  and an upper volume  $V_m$ , accounts for the observed permittivity phenomenology of relaxors. In their derivation the activation energy of the cluster is proportional to the cluster volume  $E = KV$ , and hence increasing the cluster size makes its fluctuation more difficult. The mean value of the energy distribution  $E_0$  (related to the width

(17) Viehland, D.; Jang, S.; Cross, L. E.; Wutting, M. *J. Appl. Phys.* **1990**, *68*, 2916; **1990**, *69*, 414.

(18) Lu, Z. G.; Calvarin, G. *Phys. Rev.* **1995**, *B51*, 2694.

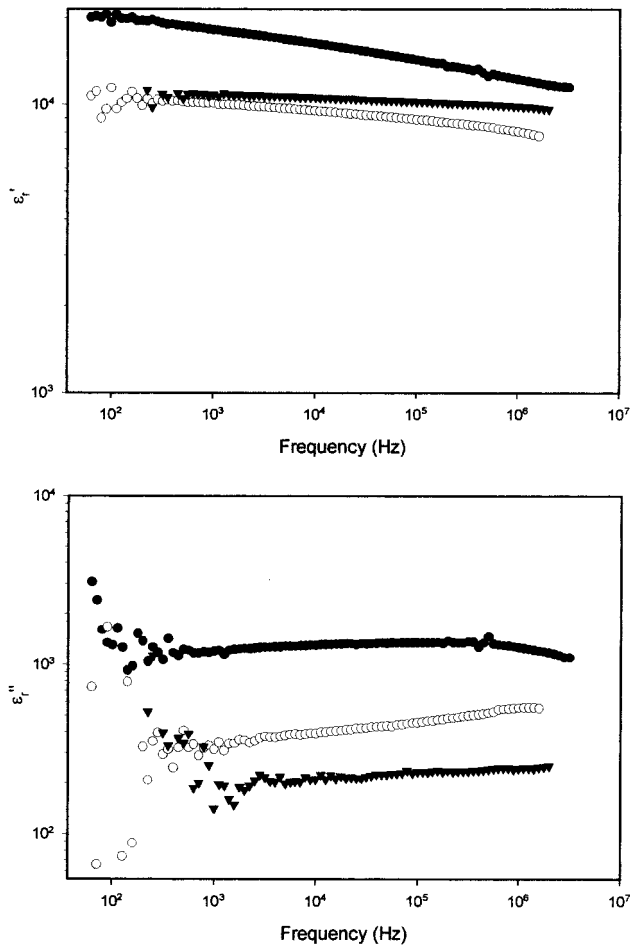


**Figure 2.** Permittivity real and imaginary parts spectra at  $T = 253$  K: (●) sample 2, (○) sample 3, and (▼) sample 4. Note the occurrence of a unique relaxation process in all samples.

of the volume distribution  $V_0$ ) results from the evaluation of the low-frequency slope of the relaxation peak  $n$  according to

$$E_0 = \frac{kT}{n}$$

in which  $k$  represents the Boltzmann constant. The evolution of  $n$  and  $E_0$  with temperature for sample 2 is shown in Figure 3. Linear behavior of  $n$  with temperature near  $T_{\max}$  in agreement with Lu and Calvarin can be observed.<sup>18</sup>  $T_0 \approx 250$  K corresponds to the temperature at which microdomains develop into macrodomains.

According to Wang and Schulze,<sup>19</sup> the low value in the dielectric constant observed in sample 4 can be assigned to the presence of PbO, detected by means of EPMA analysis. This PbO can form a layer in the grain boundary region, which dilutes the ferroelectric phase.

To explain the different dielectric behavior in the monophasic samples 2 and 3, a microstructural study has been performed.

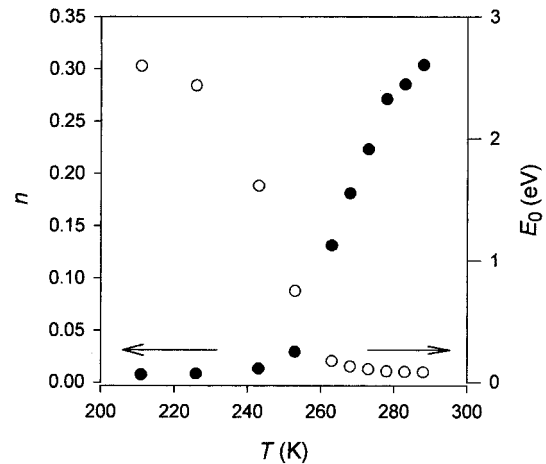


**Figure 3.** Variation of the low-frequency exponential factor  $n$  of  $\epsilon''$  spectra with temperature (●) and the corresponding mean energy of the dipolar clusters (○) for sample 2. At  $\approx 250$  K the cluster mean size undergoes a reduction.

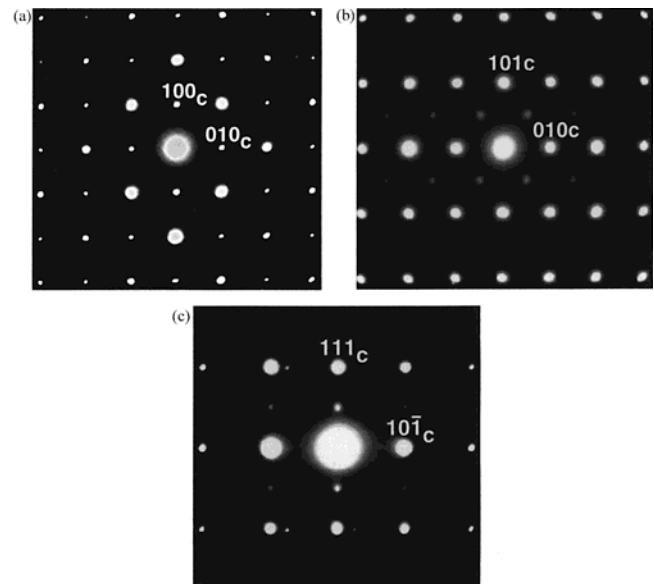


**Figure 4.** SAED pattern corresponding to sample 2 along (a)  $[001]_c$ , (b)  $[101]_c$ , and (c)  $[121]_c$ .

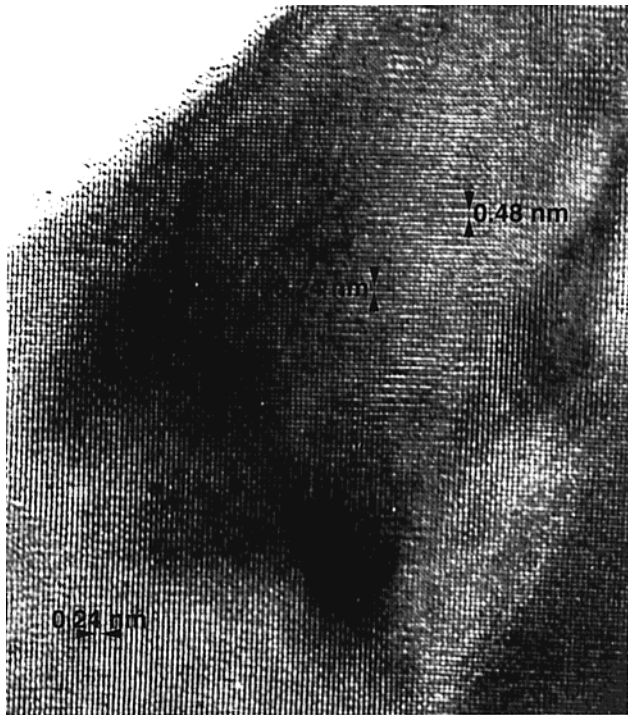
Although the X-ray diffraction pattern of sample 2 ( $\text{PbMg}_{0.33}\text{Nb}_{0.68}\text{O}_{3.02}$ ) can be assigned on the basis of a single cubic perovskite, the microstructural characterization by means of SAED and HRTEM shows a more complex situation.

Figure 4a shows the SAED pattern along the  $[001]_c$  (subindex  $c$  refers to the single cubic perovskite subcell) zone axis. All the diffraction maxima can be indexed having taken into account a single cubic perovskite subcell in agreement with the X-ray diffraction pattern. However, the SAED pattern along both the  $[101]_c$  and  $[121]_c$  zone axes, Figure 4b,c, respectively, show diffuse superlattice reflections, located at  $(\frac{1}{2} \frac{1}{2} \frac{1}{2})_c$  and equivalent reflections, suggesting a three-dimensional double perovskite unit cell ( $2a_c 2a_c 2a_c$ ). This 2-fold order is not detected by the X-ray diffraction technique, and in this sense it is also worth emphasizing the diffuse nature of the extra spots. Both structural facts suggest that the crystal must show only some ordered domains, as indeed has been observed in other oxides like  $\text{LaCaMnCoO}_6$ .<sup>20</sup>

(19) Wang, H. C.; Schulze, W. A. *J. Am. Ceram. Soc.* **1990**, *73*, 825.

(20) Vallet-Regi, M.; Garcia, E.; González-Calbet, J. M. *J. Chem. Soc., Dalton Trans.* **1988**, 775.

(21) Husson, E.; Chubb, M.; Morell, A. *Mater. Res. Bull.* **1988**, *23*, 357.



**Figure 5.** HRTEM image along  $[10\bar{1}]_c$  corresponding to sample **2**.

Figure 5 shows the HRTEM image along the  $[10\bar{1}]$  zone axis. Two different regions, marked by arrows, are observed showing (i) double and (ii) single periodicity, respectively, confirming the above proposal. Actually, small domains of double periodicity are inserted in a matrix with a simple cubic perovskite structure. These structural facts are in agreement with those previously described in the stoichiometric  $\text{PbMg}_{1/3}\text{Nb}_{2/3}\text{O}_3$ .<sup>21</sup>

Actually, regions with a double periodicity must be related to an ordered distribution of Mg and Nb cations. This would lead to a  $\text{PbMg}_{0.5}\text{Nb}_{0.5}\text{O}_3$  composition with a net negative charge, which necessarily involves positive Nb-rich regions having a simple cubic perovskite

structure. A random distribution of these small size domains (about 50 nm) makes it impossible to distinguish the superstructure by the X-ray diffraction technique. Sample **3** shows the same characteristics but there are less ordered domains in this sample than in sample **2**.

These results are in good agreement with previous microstructural studies of  $\text{PMN}^{21}$  as well as with the extended idea of the important role of the ordered Mg–Nb domains on the electric properties of this kind of material. In fact, the highest value of the dielectric constant corresponds to sample **2**, where domains of double periodicity are inserted into a cubic matrix. On the other hand, lower and similar dielectric constants have been obtained for **3** and **4** samples. These facts could indicate that the microdomain distribution has a strong influence for obtaining a good relaxor material based on the PMN structure, independent of the presence of PbO.

### Conclusions

The sol–gel method has been shown to be successful for obtaining PMN as a single phase, which is difficult to stabilize by conventional solid-state reaction. Sample **2** exhibits good relaxor behavior while worse results were obtained for samples **3** and **4**. Microstructural characterization has revealed the presence, in sample **2**, of double periodicity microdomains, suggesting Mg–Nb ordered domains, inserted in a Nb-rich cubic matrix. However, an average cubic phase seems to be the majority in samples **3** and **4**. Moreover, PbO was detected in sample **4** as an impurity phase.

Differences in microstructure seem to be responsible for the differences observed in the dielectric constants corresponding to samples **2** and **3**. This observation is supported by the fact that despite samples **2** and **3** being single phases of PMN, only sample **2**, the one with a Pb:(Mg + Nb) and Mg:Nb ratios close to 1 and 0.5, respectively, shows the highest permittivity value.

CM0011108